

Research Article

Open Access

Sarmila Sahoo*

Free vibration behavior of laminated composite stiffened elliptic parabolic shell panel with cutout

Abstract: In this paper free vibration behavior of laminated composite stiffened elliptic parabolic shell has been analyzed in terms of natural frequency and mode shape. Finite element method has been applied using an eight-noded curved quadratic isoparametric element for shell with a three noded curved beam element for stiffener. Cross and angle ply shells with different edge conditions have been studied varying the size and position of the cutouts to arrive at a set of inferences of practical engineering significances.

Keywords: laminated composites; elliptic parabolic shell; cutout; stiffener; free vibration; finite element

DOI 10.1515/cls-2015-0009

Received December 22, 2014; accepted January 15, 2015


1 Introduction

The analysis of thin shells attracted attention of researchers from the first half of the nineteenth century. While the theory of shell structures was being improved from time to time by many researchers, another group of researchers started developing exotic materials with high strength and stiffness properties. This resulted in the use of laminated composite materials to fabricate shell forms. The researchers had realized that the configuration like folded plates, conoidal, saddle, spherical, elliptic and hyperbolic parabolic and hyper shells can offer a number of parallel advantages that suit to the requirements of the industry. In fact in industrial applications a shell may have complicated boundary conditions and may be subjected to complex loading. The advent of high speed computers in the second half of the twentieth century was a major development which paved the way of researchers to get involved in analysis and design of shells of arbitrary geometry and loading conditions using numerical techniques. Ghosh

and Bandyopadhyay [1], Dey et al. [2, 3], Chakravorty et al. [4, 5] reported static and dynamic behaviour of laminated doubly curved shells. Later Nayak and Bandyopadhyay [6–8], Das and Chakravorty [9–12] and Pradyumna and Bandyopadhyay [12–14] reported static, dynamic and instability behavior of laminated doubly curved shells. The shell surfaces are often provided with cutouts for various functional requirements. Such shells need to be stiffened for avoiding stress concentration around cutouts. As the numerical approaches like finite element method become popular, investigators started venturing to analyze stiffened shells with cutout. Earlier studies in this aspect were due to Reddy [15], Malhotra et al. [16] and Sivasubramonian et al. [17]. They analyzed the effect of cutouts on the natural frequencies of plates. Later Sivakumar et al. [18], Rossi [19], Huang and Sakiyama [20] and Hota and Padhi [21] studied free vibration of plate with various cutout geometries. Researchers like, Chakravorty et al. [22], Sivasubramonian et al. [23], Hota and Chakravorty [24], Nanda and Bandyopadhyay [25] published useful information about free vibration of shells with cutout.

Shells of double curvature, particularly elliptic paraboloids, have the ability to span over relatively large distances without the need of intermediate supports in comparison with flat plates and cylindrical panels of the same general proportions. This aspect in particular attracts the designers to use such shell forms in places of large column free areas. Moreover, elliptic parabolic shells are both architecturally acceptable and structurally stiff due to their surface geometry. Qatu et al. [26] reviewed the work done on the vibration aspects of composite shells between 2000–2009 and observed that most of the researchers dealt with closed cylindrical shells. Other shell geometries like conical shells and shallow shells on rectangular, triangular, trapezoidal, circular, elliptical, rhombic or other planforms are receiving considerable attention. Recently, Kumar et al. [27–30] considered finite element formulation for shell analysis based on higher order zigzag theory. Vibration analysis of spherical shells and panels both shallow and deep has also been reported for different boundary conditions [31–34]. A complete and general view on mathematical modeling of laminated

*Corresponding Author: Sarmila Sahoo: Department of Civil Engineering, Heritage Institute of Technology, Kolkata 700107, India, E-mail: sarmila.sahoo@gmail.com, sarmila_ju@yahoo.com

 © 2015 S. Sahoo, licensee De Gruyter Open.

This work is licensed under the Creative Commons Attribution-NonCommercial-NoDerivs 3.0 License.

composite shells using higher order formulations has been provided in recent literature [35–37]. Also a wide range of literature is available on plates and shells of varying materials and geometries both in presence and absence of cutout [38–47]. However, the information for free vibration behavior of stiffened elliptic parabolic shells with cutouts is missing in literature and an in depth study of such shells in presence of cutout is needed to exploit the potential of these shell forms.

2 Mathematical Formulation

A laminated composite shell of uniform thickness h and having principal radii of curvature R_{xx} and R_{yy} (Fig. 1) is considered. Keeping the total thickness the same, the thickness may consist of any number of thin laminae each of which may be arbitrarily oriented at an angle θ with reference to the x -axis of the co-ordinate system. The constitutive equations for the shell are given by (Definitions of symbols are given in list of notations):

$$\{F\} = [E]\{\varepsilon\} \tag{1}$$

where,

$$\{F\} = \{N_x, N_y, N_{xy}, M_x, M_y, M_{xy}, Q_x, Q_y\}^T, \{\varepsilon\} = \{\varepsilon_x^0, \varepsilon_y^0, \gamma_{xy}^0, k_x, k_y, k_{xy}, \gamma_{xz}^0, \gamma_{yz}^0\}^T,$$

and

$$[E] = \begin{bmatrix} A_{11} & A_{12} & A_{16} & B_{11} & B_{12} & B_{16} & 0 & 0 \\ A_{12} & A_{22} & A_{26} & B_{12} & B_{22} & B_{26} & 0 & 0 \\ A_{16} & A_{26} & A_{66} & B_{16} & B_{26} & B_{66} & 0 & 0 \\ B_{11} & B_{12} & B_{16} & D_{11} & D_{12} & D_{16} & 0 & 0 \\ B_{12} & B_{22} & B_{26} & D_{12} & D_{22} & D_{26} & 0 & 0 \\ B_{16} & B_{26} & B_{66} & D_{16} & D_{26} & D_{66} & 0 & 0 \\ 0 & 0 & 0 & 0 & 0 & 0 & S_{11} & S_{12} \\ 0 & 0 & 0 & 0 & 0 & 0 & S_{12} & S_{22} \end{bmatrix}$$

The detailed expressions of the elements of the elasticity matrix are available in several references including Vasiliev et al. [48] and Qatu [49]. The elements of the stiffness matrix $[E]$ are defined as

$$A_{ij} = \sum_{k=1}^{np} (Q_{ij})_k (z_k - z_{k-1}),$$

$$B_{ij} = \frac{1}{2} \sum_{k=1}^{np} (Q_{ij})_k (z_k^2 - z_{k-1}^2),$$

$$D_{ij} = \frac{1}{3} \sum_{k=1}^{np} (Q_{ij})_k (z_k^3 - z_{k-1}^3) \quad i, j = 1, 2, 6,$$

and $S_{ij} = \sum_{k=1}^{np} F_i F_j (G_{ij})_k (z_k - z_{k-1}) \quad i, j = 4, 5.$

In the above equations z_k and z_{k-1} are the distances measured from the mid surface of a laminate to the bottom of

the k th and $(k-1)$ th laminate, respectively. np is the number of plies in a laminate. Q_{ij} are elements of the off-axis elastic constant matrix which is given by

$$[Q_{ij}]_{off} = [T_1]^{-1} [Q_{ij}]_{on} [T_1]^{-T}, \quad i, j = 1, 2, 6,$$

and $[G_{ij}]_{off} = [T_2]^{-1} [Q_{ij}]_{on} [T_2], \quad i, j = 4, 5.$

$$[T_1] = \begin{bmatrix} m^2 & n^2 & 2mn \\ n^2 & m^2 & -2mn \\ -mn & mn & m^2 - n^2 \end{bmatrix}, \quad [T_2] =$$

$$= \begin{bmatrix} m & -n \\ n & m \end{bmatrix}, \text{ in which } m = \cos \theta \text{ and } n = \sin \theta.$$

$$[Q_{ij}]_{on} = \begin{bmatrix} Q_{11} & Q_{12} & 0 \\ Q_{12} & Q_{22} & 0 \\ 0 & 0 & Q_{66} \end{bmatrix}, \quad i, j = 1, 2, 6,$$

and $[Q_{ij}]_{on} = \begin{bmatrix} Q_{44} & 0 \\ 0 & Q_{55} \end{bmatrix}, \quad i, j = 4, 5.$

In which, $Q_{11} = (1 - \nu_{12}\nu_{21})^{-1}E_{11}$, $Q_{22} = (1 - \nu_{12}\nu_{21})^{-1}E_{22}$, $Q_{12} = (1 - \nu_{12}\nu_{21})^{-1}E_{11}\nu_{21}$, $Q_{44} = G_{13}$, $Q_{55} = G_{23}$, $Q_{66} = G_{12}$.

F_i and F_j are two factors presently taken as unity for thin shells. When the shell is moderately thick, the product of F_i and F_j is taken as 5/6, which is commonly used since the evaluation of shear correction factor from exact theory of elasticity is difficult.

The stress-strain relations are given by

$$\begin{Bmatrix} \sigma_x \\ \sigma_y \\ \tau_{xy} \end{Bmatrix} = \begin{bmatrix} Q_{11} & Q_{12} & Q_{16} \\ Q_{12} & Q_{22} & Q_{26} \\ Q_{16} & Q_{26} & Q_{66} \end{bmatrix} \begin{Bmatrix} \varepsilon_x^0 \\ \varepsilon_y^0 \\ \varepsilon_{xy}^0 \end{Bmatrix} + z \begin{Bmatrix} k_x \\ k_y \\ k_{xy} \end{Bmatrix} \tag{2}$$

$$\text{and } \begin{Bmatrix} \tau_{xz} \\ \tau_{yz} \end{Bmatrix} = \begin{bmatrix} Q_{44} & Q_{45} \\ Q_{45} & Q_{55} \end{bmatrix} \begin{Bmatrix} \gamma_{xz}^0 \\ \gamma_{yz}^0 \end{Bmatrix} \tag{3}$$

where, $Q_{45} = (G_{13} - G_{23})mn$.

The force and moment resultants are expressed as

$$\begin{Bmatrix} N_x, N_y, N_{xy}, M_x, M_y, M_{xy}, Q_x, Q_y \end{Bmatrix}^T = \int_{-h/2}^{h/2} \begin{Bmatrix} \sigma_x, \sigma_y, \tau_{xy}, \sigma_z, \dots \\ \dots \sigma_y, z, \tau_{xy}, z, \tau_{xz}, \tau_{yz} \end{Bmatrix}^T dz \tag{4}$$

The strain-displacement relations on the basis of improved first order approximation theory for thin shell [50] are established as

$$\begin{Bmatrix} \varepsilon_x, \varepsilon_y, \gamma_{xy}, \gamma_{xz}, \gamma_{yz} \end{Bmatrix}^T = \begin{Bmatrix} \varepsilon_x^0, \varepsilon_y^0, \gamma_{xy}^0, \gamma_{xz}^0, \gamma_{yz}^0 \end{Bmatrix}^T + z \begin{Bmatrix} k_x, k_y, k_{xy}, k_{xz}, k_{yz} \end{Bmatrix}^T \tag{5}$$

where, the first vector is the mid-surface strain for a shell and the second vector is the curvature and are related to degrees of freedom as:

$$\begin{Bmatrix} \epsilon_x^0 \\ \epsilon_y^0 \\ \gamma_{xy}^0 \\ \gamma_{xz}^0 \\ \gamma_{yz}^0 \end{Bmatrix} = \begin{Bmatrix} \partial u/\partial x - w/R_{xx} \\ \partial v/\partial y - w/R_{yy} \\ \partial u/\partial y + \partial v/\partial x - 2w/R_{xy} \\ \alpha + \partial w/\partial x \\ \beta + \partial w/\partial y \end{Bmatrix} \quad (6)$$

and

$$\begin{Bmatrix} k_x \\ k_y \\ k_{xy} \\ k_{xz} \\ k_{yz} \end{Bmatrix} = \begin{Bmatrix} \partial \alpha/\partial x \\ \partial \beta/\partial y \\ \partial \alpha/\partial y + \partial \beta/\partial x \\ 0 \\ 0 \end{Bmatrix} \quad (7)$$

Finite Element Formulation

An eight-noded curved quadratic isoparametric finite element is used for shell analysis. Any shell surface can be modeled by three dimensional solid elements. When the thickness dimension is considerably smaller than the other dimensions, the nodes along the thickness direction supply additional degrees of freedom than needed and hence are not preferred. When a two dimensional element is obtained by considering the thickness direction nodes, the displacements of adjacent thickness direction nodes must be ensured to be equal to avoid numerical difficulties. Thus the five degrees of freedom including three translations (u, v, w) and two rotations (α, β) are attached to each node. The final element has mid surface nodes only and a line in the thickness direction remains straight but not necessarily normal to the mid surface after deformation. The directions of the generalized displacements are shown in Fig. 1. The following expressions establish the relations between the displacement at any point with respect to the co-ordinates ζ and η and the nodal degrees of freedom.

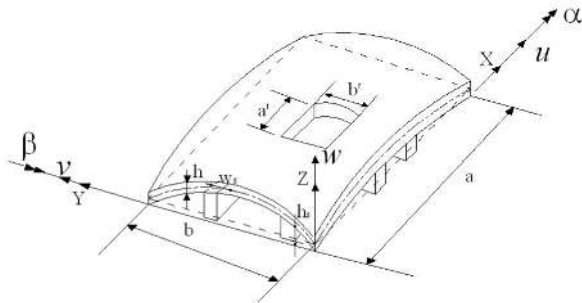


Figure 1: Elliptic parabolic shell with a concentric cutout stiffened along the margins

$$\begin{aligned} u &= \sum_{i=1}^8 N_i u_i & v &= \sum_{i=1}^8 N_i v_i & w &= \sum_{i=1}^8 N_i w_i \\ \alpha &= \sum_{i=1}^8 N_i \alpha_i & \beta &= \sum_{i=1}^8 N_i \beta_i \end{aligned} \quad (8)$$

where the shape functions derived from a cubic interpolation polynomial are:

$$\begin{aligned} N_i &= (1 + \zeta \zeta_i)(1 + \eta \eta_i)(\zeta \zeta_i + \eta \eta_i - 1)/4, \\ &\quad \text{for } i = 1, 2, 3, 4 \\ N_i &= (1 + \zeta \zeta_i)(1 - \eta^2)/2, \quad \text{for } i = 5, 7 \\ N_i &= (1 + \eta \eta_i)(1 - \zeta^2)/2, \quad \text{for } i = 6, 8 \end{aligned} \quad (9)$$

The generalized displacement vector of an element is expressed in terms of the shape functions and nodal degrees of freedom as:

$$[u] = [N] \{d_e\} \quad (10)$$

$$\{u\} = \begin{Bmatrix} u \\ v \\ w \\ \alpha \\ \beta \end{Bmatrix} =$$

i.e.,

$$= \sum_{i=1}^8 \begin{bmatrix} N_i & & & & \\ & N_i & & & \\ & & N_i & & \\ & & & N_i & \\ & & & & N_i \end{bmatrix} \begin{Bmatrix} u_i \\ v_i \\ w_i \\ \alpha_i \\ \beta_i \end{Bmatrix}$$

Element Stiffness Matrix

The strain-displacement relation is given by

$$\{\epsilon\} = [B] \{d_e\}, \quad (11)$$

$$\text{where } [B] = \sum_{i=1}^8 \begin{bmatrix} N_{i,x} & 0 & -\frac{N_i}{R_{xx}} & 0 & 0 \\ 0 & N_{i,y} & -\frac{N_i}{R_{yy}} & 0 & 0 \\ N_{i,y} & N_{i,x} & -\frac{2N_i}{R_{xy}} & 0 & 0 \\ 0 & 0 & 0 & N_{i,x} & 0 \\ 0 & 0 & 0 & 0 & N_{i,y} \\ 0 & 0 & 0 & N_{i,y} & N_{i,x} \\ 0 & 0 & N_{i,x} & N_i & 0 \\ 0 & 0 & N_{i,y} & 0 & N_i \end{bmatrix} \quad (12)$$

The element stiffness matrix is

$$[K_e] = \iint [B]^T [E] [B] dx dy \quad (13)$$

Element Mass Matrix

The element mass matrix is obtained from the integral

$$[M_e] = \iint [N]^T [P] [N] dx dy, \quad (14)$$

where,

$$[N] = \sum_{i=1}^8 \begin{bmatrix} N_i & 0 & 0 & 0 & 0 \\ 0 & N_i & 0 & 0 & 0 \\ 0 & 0 & N_i & 0 & 0 \\ 0 & 0 & 0 & N_i & 0 \\ 0 & 0 & 0 & 0 & N_i \end{bmatrix},$$

$$[P] = \sum_{i=1}^8 \begin{bmatrix} P & 0 & 0 & 0 & 0 \\ 0 & P & 0 & 0 & 0 \\ 0 & 0 & P & 0 & 0 \\ 0 & 0 & 0 & I & 0 \\ 0 & 0 & 0 & 0 & I \end{bmatrix},$$

in which $P = \sum_{k=1}^{np} \int_{z_{k-1}}^{z_k} \rho dz$ and $I = \sum_{k=1}^{np} \int_{z_{k-1}}^{z_k} z \rho dz$ (15)

where np is the number of plies in a laminate.

Finite Element Formulation for Stiffener of the Shell

Three noded curved isoparametric beam elements (Fig. 2) are used to model the stiffeners, which are taken to run only along the boundaries of the shell elements. In the stiffener element, each node has four degrees of freedom i.e. u_{sx}, w_{sx}, a_{sx} and b_{sx} for x -stiffener and v_{sy}, w_{sy}, a_{sy} and b_{sy} for y -stiffener. The generalized force-displacement relation of stiffeners can be expressed as:

x -stiffener : $\{F_{sx}\} = [D_{sx}] \{\epsilon_{sx}\} = [D_{sx}] [B_{sx}] \{\delta_{sxi}\};$
 y -stiffener : $\{F_{sy}\} = [D_{sy}] \{\epsilon_{sy}\} = [D_{sy}] [B_{sy}] \{\delta_{syi}\}$ (16)

where, $\{F_{sx}\} = [N_{sxx} \ M_{sxx} \ T_{sxx} \ Q_{sxxz}]^T;$
 $\{\epsilon_{sx}\} = [u_{sx,x} \ \alpha_{sx,x} \ \beta_{sx,x} \ (\alpha_{sx} + w_{sx,x})]^T$
 and $\{F_{sy}\} = [N_{syy} \ M_{syy} \ T_{syy} \ Q_{syyz}]^T;$
 $\{\epsilon_{sy}\} = [v_{sy,y} \ \beta_{sy,y} \ \alpha_{sy,y} \ (\beta_{sy} + w_{sy,y})]^T$

The generalized displacements of the x -stiffener and the shell are related by the transformation matrix $\{\delta_{sxi}\} = [T_x] \{\delta\}$ where

$$[T_x] = \begin{bmatrix} 1 + \frac{e}{R_{xx}} & \text{symmetric} & & \\ 0 & 1 & & \\ 0 & 0 & 1 & \\ 0 & 0 & 0 & 1 \end{bmatrix} \quad (17)$$

The generalized displacements of the y -stiffener and the shell are related by the transformation matrix $\{\delta_{syi}\} = [T_y] \{\delta\}$ where

$$[T_y] = \begin{bmatrix} 1 + \frac{e}{R_{yy}} & \text{symmetric} & & \\ 0 & 1 & & \\ 0 & 0 & 1 & \\ 0 & 0 & 0 & 1 \end{bmatrix} \quad (18)$$

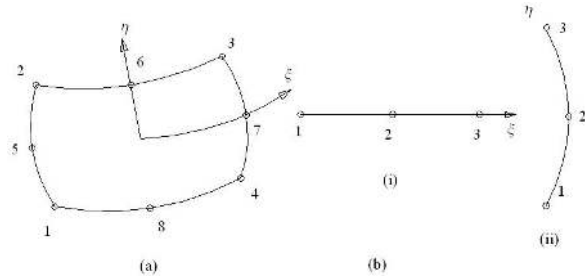


Figure 2: (a) Eight noded shell element with isoparametric coordinates (b) Three noded stiffener elements (i) x -stiffener (ii) y -stiffener

These transformations are required due to curvature of x -stiffener and y -stiffener. In the above equations, e is the eccentricity of the stiffeners. $\{\delta\}$ is the appropriate portion of the displacement vector of the shell excluding the displacement component along the other axis.

Elasticity matrices are as follows:

$$[D_{sx}] = \begin{bmatrix} A_{11} b_{sx} & B'_{11} b_{sx} & B'_{12} b_{sx} & 0 \\ B'_{11} b_{sx} & D'_{11} b_{sx} & D'_{12} b_{sx} & 0 \\ B'_{12} b_{sx} & D'_{12} b_{sx} & \frac{1}{6} (Q_{44} + Q_{66}) d_{sx} b_{sx}^3 & 0 \\ 0 & 0 & 0 & b_{sx} S_{11} \end{bmatrix} \quad (19)$$

$$[D_{sy}] = \begin{bmatrix} A_{22} b_{sy} & B'_{22} b_{sy} & B'_{12} b_{sy} & 0 \\ B'_{22} b_{sy} & \frac{1}{6} (Q_{44} + Q_{66}) b_{sy} & D'_{12} b_{sy} & 0 \\ B'_{12} b_{sy} & D'_{12} b_{sy} & D'_{11} d_{sy} b_{sy}^3 & 0 \\ 0 & 0 & 0 & b_{sy} S_{22} \end{bmatrix} \quad (20)$$

where,

$$D'_{ij} = D_{ij} + 2eB_{ij} + e^2 A_{ij}; \quad B'_{ij} = B_{ij} + eA_{ij}, \quad (21)$$

and A_{ij}, B_{ij}, D_{ij} and S_{ij} are explained in literature [51].

Here for the stiffener considering it as moderately thick, the shear correction factor is taken as $5/6$. The sectional parameters are calculated with respect to the mid-surface of the shell by which the effect of eccentricities of stiffeners is automatically included. The element stiffness matrices are of the following forms.

for x -stiffener : $[K_{xe}] = \int [B_{sx}]^T [D_{sx}] [B_{sx}] dx;$
 for y -stiffener : $[K_{ye}] = \int [B_{sy}]^T [D_{sy}] [B_{sy}] dy$ (22)

The integrals are converted to isoparametric coordinates and are carried out by 2-point Gauss quadrature. Finally, the element stiffness matrix of the stiffened shell is obtained by appropriate matching of the nodes of the stiffener and shell elements through the connectivity matrix

and is given as:

$$[K_e] = [K_{she}] + [K_{xe}] + [K_{ye}] \tag{23}$$

The element stiffness matrices are assembled to get the global matrices.

Element Mass Matrix

The element mass matrix for shell is obtained from the integral

$$[M_e] = \iint [N]^T [P] [N] dx dy, \tag{24}$$

where,

$$[N] = \sum_{i=1}^8 \begin{bmatrix} N_i & 0 & 0 & 0 & 0 \\ 0 & N_i & 0 & 0 & 0 \\ 0 & 0 & N_i & 0 & 0 \\ 0 & 0 & 0 & N_i & 0 \\ 0 & 0 & 0 & 0 & N_i \end{bmatrix},$$

$$[P] = \sum_{i=1}^8 \begin{bmatrix} P & 0 & 0 & 0 & 0 \\ 0 & P & 0 & 0 & 0 \\ 0 & 0 & P & 0 & 0 \\ 0 & 0 & 0 & I & 0 \\ 0 & 0 & 0 & 0 & I \end{bmatrix},$$

$$\text{in which } P = \sum_{k=1}^{np} \int_{z_{k-1}}^{z_k} \rho dz \text{ and } I = \sum_{k=1}^{np} \int_{z_{k-1}}^{z_k} z^2 \rho dz \tag{25}$$

where np is the number of plies in a laminate.

Element mass matrix for stiffener element

$$[M_{sx}] = \int [N]^T [P] [N] dx \text{ for } x\text{-stiffener}$$

$$\text{and } [M_{sy}] = \int [N]^T [P] [N] dy \text{ for } y\text{-stiffener} \tag{26}$$

Here, $[N]$ is a 3×3 diagonal matrix for stiffener.

$$[P] = \sum_{i=1}^3 \begin{bmatrix} \rho \cdot b_{sx} d_{sx} & 0 & 0 \\ 0 & \rho \cdot b_{sx} d_{sx} & 0 \\ 0 & 0 & \rho \cdot b_{sx} d_{sx}^2 / 12 \dots \\ 0 & 0 & 0 \end{bmatrix} \dots$$

$$\left. \begin{matrix} 0 \\ 0 \\ 0 \\ \rho(b_{sx} \cdot d_{sx}^3 + b_{sx}^3 \cdot d_{sx}) / 12 \end{matrix} \right\} \text{for } x\text{-stiffener}$$

$$[P] = \sum_{i=1}^3 \begin{bmatrix} \rho \cdot b_{sy} d_{sy} & 0 & 0 \\ 0 & \rho \cdot b_{sy} d_{sy} & 0 \\ 0 & 0 & \rho \cdot b_{sy} d_{sy}^2 / 12 \dots \\ 0 & 0 & 0 \end{bmatrix} \dots$$

$$\left. \begin{matrix} 0 \\ 0 \\ 0 \\ \rho(b_{sy} \cdot d_{sy}^3 + b_{sy}^3 \cdot d_{sy}) / 12 \end{matrix} \right\} \text{for } y\text{-stiffener}$$

The mass matrix of the stiffened shell element is the sum of the matrices of the shell and the stiffeners matched at the appropriate nodes.

$$[M_e] = [M_{she}] + [M_{xe}] + [M_{ye}] \tag{27}$$

The element mass matrices are assembled to get the global matrices.

Modeling the cutout

The code developed can take the position and size of cutout as input. The program is capable of generating non uniform finite element mesh all over the shell surface. So the element size is gradually decreased near the cutout margins. One such typical mesh arrangement is shown in Fig. 3 where the mesh divisions are in the ratio 6:4:4:3:3:3:3:4:4:6. Such finite element mesh is redefined in steps and a particular grid is chosen to obtain the fundamental frequency when the result does not improve by more than one percent on further refining. Convergence of results is ensured in all the problems taken up here.

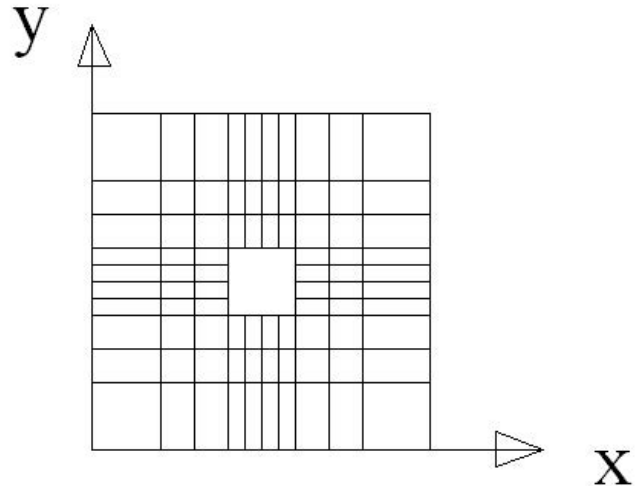


Figure 3: Typical 10x10 non-uniform mesh arrangements drawn to scale

Solution Procedure for Free Vibration Analysis

The free vibration analysis involves determination of natural frequencies from the condition

$$|[K] - \omega^2 [M]| = 0 \tag{28}$$

Table 1: Natural frequencies (Hz) of centrally stiffened clamped square plate

Mode no.	Mukherjee and Mukhopadhyay [52]	Nayak and Bandyopadhyay [53]		Present method
		N8 (FEM)	N9 (FEM)	
1	711.8	725.2	725.1	733

$a = b = 0.2032$ m, shell thickness = 0.0013716 m, stiffener depth 0.0127 m, stiffener width = 0.00635 m, stiffener eccentric at bottom
 Material property: $E = 6.87 \times 10^{10}$ N/m², $\nu = 0.29$, $\rho = 2823$ kg/m³

Table 2: Non-dimensional Fundamental Frequencies ($\bar{\omega}$) for laminated composite saddle shell with cutout.

a'/a	CS		SS		CL	
	Chakravorty et al. [22]	Present model	Chakravorty et al. [22]	Present model	Chakravorty et al. [22]	Present model
0.0	13.485	13.249	14.721	14.686	113.567	112.926
0.1	13.060	13.084	14.350	14.695	97.753	98.041
0.2	12.530	12.449	13.544	13.507	97.599	97.032
0.3	12.016	12.038	12.908	12.882	111.489	111.033
0.4	11.721	11.733	12.560	12.559	110.210	110.20

$a/b = 1$, $a/h = 100$, $a'/b' = 1$, $h/R_{xx} = -h/R_{yy} = 1/300$,
 CS=Corner point supported, SS=Simply supported, CL=Clamped

Table 3: Non-dimensional Fundamental Frequencies ($\bar{\omega}$) for laminated composite (0/90/0/90) stiffened elliptic parabolic shell for different sizes of the central square cutout and different boundary conditions.

Boundary conditions	Cutout size (a'/a)				
	0	0.1	0.2	0.3	0.4
CCCC	139.71	119.13	133.82	152.26	152.99
CSCC	98	105.54	117.64	120.51	121.84
CCSC	99.19	106.35	118.08	129.78	133.29
CCCS	97.8	104.59	117.34	120.5	121.82
CSSC	80.43	87.38	92.46	96.68	100.71
CCSS	80.43	87.38	92.46	96.68	100.71
CSCS	106.82	100.62	113.02	113.71	114.7
SCSC	100.3	103.75	115.68	124.68	125.6
CSSS	72.96	80.66	83.91	87.7	92.14
SSSC	75.27	82.63	86.14	89.89	93.65
SSCS	72.96	79.7	83.91	87.7	92.14
SSSS	66.29	72.77	76.75	80.43	84.75
Point supported	35.65	38.04	40.62	43.15	42.99

$a/b = 1$, $a/h = 100$, $a'/b' = 1$, $h/R_{xx} = 1/300$, $R_{xx}/R_{yy} = 1.5$;
 $E_{11}/E_{22} = 25$, $G_{23} = 0.2 E_{22}$, $G_{13} = G_{12} = 0.5 E_{22}$, $\nu_{12} = \nu_{21} = 0.25$.

Table 4: Non-dimensional Fundamental Frequencies ($\bar{\omega}$) for laminated composite (+45/-45/+45/-45) stiffened elliptic parabolic shell for different sizes of the central square cutout and different boundary conditions.

Boundary conditions 0	Cutout size (a'/a)				
	0.1	0.2	0.3	0.4	
CCCC	143.55	156.08	165.22	166.77	157.25
CSCC	118.68	127.5	129.9	130.18	126.45
CCSC	127.22	135.27	139.29	140.28	138.42
CCCS	118.65	127.28	129.87	129.98	126.43
CSSC	112.52	122.38	124.23	124.1	121.69
CCSS	112.58	122.42	124.66	124.11	121.12
CSCS	108.89	117.52	122.31	126.27	125.59
SCSC	118.85	127.01	133.74	139.51	136.51
CSSS	102.38	111.57	115.4	118.74	119.75
SSSC	107.64	117.59	119.26	118.89	116.87
SSCS	102.37	111.77	115.4	118.74	119.75
SSSS	96.82	106.74	109.73	112.61	114.3
Point supported	32.82	35.56	38.02	41.03	42.2

$a/b = 1, a/h = 100, a'/b' = 1, h/R_{xx} = 1/300, R_{xx}/R_{yy} = 1.5;$
 $E_{11}/E_{22} = 25, G_{23} = 0.2 E_{22}, G_{13} = G_{12} = 0.5 E_{22}, \nu_{12} = \nu_{21} = 0.25.$

Table 5: Clamping options for 0/90/0/90 elliptic parabolic shells with central cutouts having a'/a ratio 0.2.

Number of sides to be clamped	Clamped edges	Improvement of frequencies with respect to point supported shells	Marks indicating the efficiencies of no of restraints
0	Corner Point supported	-	0
0	Simply supported no edges clamped (SSSS)	Good improvement	39
1	a) Elliptic edge along $x = a$ (SSCS)	Good improvement	46
	b) Elliptic edge along $x = 0$ (CSSS)	Good improvement	46
	b) One parabolic edge along $y = b$ (SSSC)	Good improvement	49
2	a) Two elliptic edges $x = 0$ and $x = a$ (CSCS)	Marked improvement	78
	b) Two parabolic edges along $y = 0$ and $y = b$ (SCSC)	Marked improvement	81
	c) Any two adjacent edges (CSSC, CCSS)	Good improvement	56
3	3 edges including the two elliptic edges (CSCC, CCCS)	Marked improvement	83
	3 edges excluding the elliptic edge along $x = a$ (CCSC)	Marked improvement	83
4	All sides (CCCC)	Frequency attains highest value	100

This is a generalized eigen value problem and is solved by the subspace iteration algorithm. The generalized formulation considers all three radii of curvature, viz., R_{xx} , R_{yy} and R_{xy} . The shell surface considered for the present study is elliptic parabolic which has the following features and can be handled by the proposed formulation as a special case: doubly curved synclastic surface having $R_{xx}/R_{yy} = 1.5$ and $1/R_{xy} = 0$.

3 Results and discussion

Numerical results are obtained by employing an appropriate mesh size until the convergence is achieved with a residual error below 1%. The accuracy of the formulation is first established by comparing the results of the present analysis with those existing in the literature. Non-dimensional frequencies for centrally stiffened clamped square plate obtained through present formulation are compared with those of Mukherjee and Mukhopadhyay [52] and Nayak and Bandyopdhyay [53] as furnished in Table 1. Here for comparison, a shell has been converted to a plate considering a high value of radius of curvature. The agreement is found to be good. This establishes the correctness of stiffener formulation. The present FEM results are also compared with those obtained by Chakravorty et al. [22] for corner point supported, simply supported and clamped laminated composite saddle shells with cutouts. These are presented in Table 2 and the results are found to match extremely well. Thus the cutout formulation for doubly curved shell is established.

Numerical results are then obtained for several elliptic parabolic shells with 0/90/0/90 and +45/-45/+45/-45 laminations by varying boundary constraints, cutout size and position. The shell thickness h is taken to be constant in all cases and lamina properties taken are: $E_{11}/E_{22} = 25$, $G_{23} = 0.2 E_{22}$, $G_{13} = G_{12} = 0.5 E_{22}$, $\nu_{12} = \nu_{21} = 0.25$.

Tables 3 and 4 contains the results of non-dimensional frequency ($\bar{\omega}$) of 0/90/0/90 and +45/-45/+45/-45 stiffened elliptic parabolic shells of square planform with cutouts. The cutouts are also taken to be square in plan ($a' = b'$). The sizes of the concentric cutouts are varied from 0 to 0.4 and boundary conditions are varied along the four edges. The stiffeners, along the cutout periphery are extended up to the edge of the shell. The boundary conditions are designated as: C for clamped and S for simply supported. The four edges are considered in an anticlockwise order from the edge $x = 0$. For example a shell with CSCS boundary is clamped along $x = 0$, simply supported along $y = 0$

and clamped along $x = a$ and simply supported along $y = b$.

The effect of cutout size on fundamental frequency of composite shells with different boundary conditions can be studied using the results furnished in Tables 3 and 4. All the stiffened shells exhibit greater stiffness with introduction of cutout. But in some angle ply shell, the frequency shows a monotonic increase upto $a'/a = 0.3$. This initial increase in frequency is due to the fact that with the introduction of cutout, numbers of stiffeners are increase from two to four in the present study. Only one exception is there. In case of clamped shell, with the introduction of cutout, fundamental frequency decreases. In this case, though number of stiffeners increases but loss of stiffness is relatively more pronounced. Table 3 and 4 provides further information about the effect of cutout size on fundamental frequency. With further increase in cutout size, the shell surface undergoes loss of both mass and stiffness as a result fundamental frequency may increase or decrease. As with the introduction of a cutout of $a'/a = 0.3$, in shell surface, the frequency increases in all the cases, this leads to the engineering conclusion that concentric cutouts with stiffened margins may be provided safely on shell surfaces for corner point supported functional requirements upto $a'/a = 0.3$.

The boundary conditions arranged according to the increased number of boundary constraints are as follows: Corner Point supported, SSSS, SSCS, SSSC, CSSS, SSSC, CSCS, SCSC, CSSC, CCSS, CSCC, CCCS, CCSC and CCCC. As evident from Tables 5 and 6, fundamental frequencies of members belonging to same number of boundary constraints may not have the same value. Stiffness depends on number of boundary constraints. Arrangement of boundary constraints are more significant than number of boundary constraints to increase the stiffness of the stiffened shells with cutout. Table 5 and 6 shows the efficiency of a particular boundary combination in increasing the fundamental frequency. Marks are assigned to each boundary combination in a scale assigning a value of 0 to the minimum frequency (corner point supported shell) and 100 to the maximum frequency (clamped shell). These marks are furnished for cutouts with $a'/a = 0.2$. These tables will enable a practicing engineer to realize at a glance the efficiency of a particular boundary combination in increasing the frequency of a shell, taking that of clamped shell as the upper limit.

It can be seen from the present study that if the one edge is released from clamped to simply supported, the change of frequency is more in case of an angle ply shells than that for a cross ply shells. Again, if the two adjacent edges are released, fundamental frequency decreases re-

Table 6: Clamping options for +45/-45/+45/-45 elliptic parabolic shells with central cutouts having a'/a ratio 0.2.

Number of sides to be clamped	Clamped edges	Improvement of frequencies with respect to point supported shells	Marks indicating the efficiencies of no of restraints
0	Corner Point supported	-	0
0	Simply supported no edges clamped (SSSS)	Good improvement	56
1	a) Elliptic edge along $x = a$ (SSCS)	Good improvement	61
	b) Elliptic edge along $x = 0$ (CSSS)	Good improvement	61
	along $y = b$ (SSSC)	Good improvement	64
	along $y = 0$ (SSSC)	Good improvement	64
2	a) Two elliptic edges $x = 0$ and $x = a$ (CSCS)	Marked improvement	66
	b) Two parabolic edges along $y = 0$ and $y = b$ (SCSC)	Marked improvement	75
	c) Any two adjacent edges (CSCC,CCSS)	Marked improvement	68
3	3 edges including the two elliptic edges (CSCC,CCCS)	Marked improvement	72
	3 edges excluding the elliptic edge along $x = a$ (CCSC)	Remarkable improvement	80
4	All sides (CCCC)	Frequency attains highest value	100

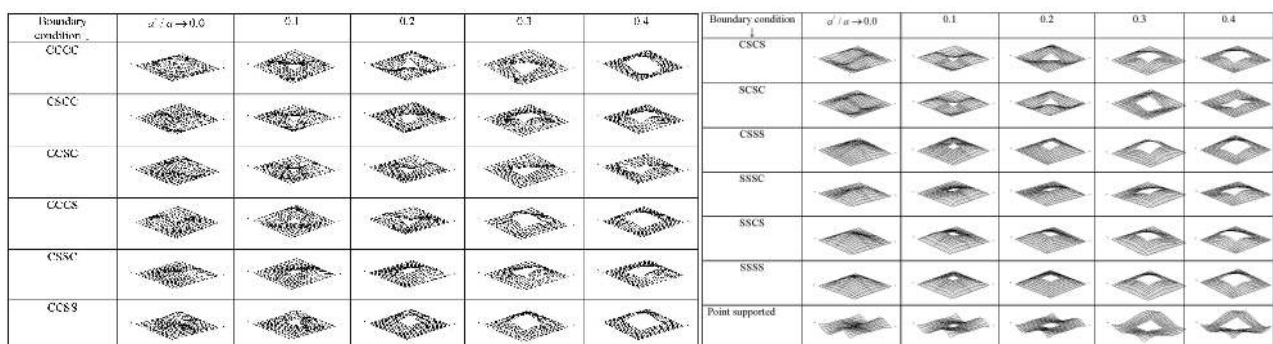


Figure 4: First mode shapes of laminated composite (0/90/0/90) stiffened elliptic parabolic shell for different sizes of the central square cutout and boundary conditions

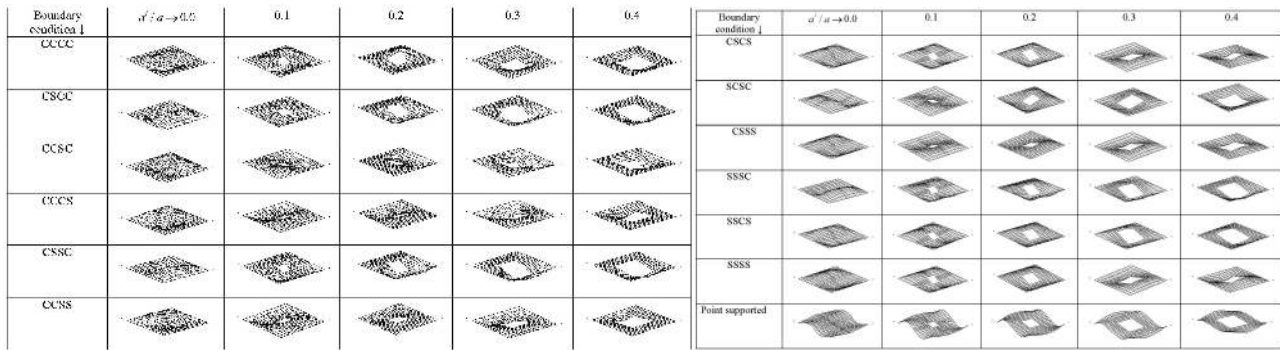


Figure 5: First mode shapes of laminated composite (+45/-45/+45/-45) stiffened elliptic parabolic shell for different sizes of the central square cutout and boundary conditions

markably whereas if the two alternate edges are released the decrease in frequency is far less. This change in frequency is very much significant in case of cross ply shells. For cross ply shells if three or four edges are simply supported, frequency values undergo marked decrease but for angle ply shells with the introduction of more number of simply supported edges the frequency value does not change so drastically. The results indicate that particularly for cross ply shells two alternate edges should preferably be clamped in order to achieve higher frequency values.

The mode shapes of the fundamental modes of vibration are shown in Fig. 4 and Fig. 5 for cross-ply and angle ply shells respectively. The normalized displacements are plotted taking the shell mid-surface as the reference. For all the boundary conditions for cross ply and angle ply shell the fundamental mode is clearly a bending mode or torsional mode. Only for corner point supported shells the fundamental mode shapes are complicated. With the introduction of cutout mode shapes remain almost similar. When the size of the cutout is increased from 0.2 to 0.4 the fundamental modes of vibration are presented.

The effect of eccentricity of cutout positions on fundamental frequencies, are studied from the results obtained for different locations of a cutout with $a'/a = 0.2$. The non-dimensional coordinates of the cutout centre ($\bar{x} = \frac{x}{a}, \bar{y} = \frac{y}{a}$) was varied from 0.2 to 0.8 along each directions, so that the distance of a cutout margin from the shell boundary was not less than one tenth of the plan dimension of the shell. The margins of cutouts were stiffened with four stiffeners. The study was carried out for all the thirteen boundary conditions for both cross ply and angle ply shells. The fundamental frequency of a shell with an eccentric cutout is expressed as a percentage of fundamental frequency of a shell with a concentric cutout. This percentage is denoted by r . In Tables 7 and 8 such results are furnished.

It can be seen that eccentricity of the cutout along the length of the shell towards the clamped edges makes it more flexible. When edge, opposite to a clamped edge is simply supported, r value first increases towards the simply supported edge then decreases. This is true for both cross ply and angle ply shells. For cross ply shells, when two opposite edges are simply supported r value decreases towards the simply supported edges. But in case of an angle ply shell, if the two opposite edges are simply supported then r value first increase and then decrease towards the boundary. So, for functional purposes, if a shift of central cutout is required, eccentricity of a cutout along the length or width should preferably be towards the simply supported edge but not towards very near to the boundary for angle ply shells. But in case of cross ply shells eccentricity of a cutout should be towards a simply supported edge, which is opposite to a clamped edge.

Tables 9 and 10 provide the maximum values of r together with the position of the cutout. These tables also show the rectangular zones within which r is always greater than or equal to 90 and 95. It is to be noted that at some other points r values may have similar values, but only the zone rectangular in plan has been identified. These tables indicate the maximum eccentricity of a cutout which can be permitted if the fundamental frequency of a concentrically punctured shell is not to reduce a drastic amount. So these tables will help practicing engineers

The mode shapes corresponding to the fundamental modes of vibration are plotted in Fig. 6 - 13 for cross-ply and angle ply shell of different boundary conditions for different eccentric position of the cutout. All the mode shapes are either bending or torsional mode. It is found that for different position of cutout mode shapes are somewhat similar to one another, only the crest and trough position changes.

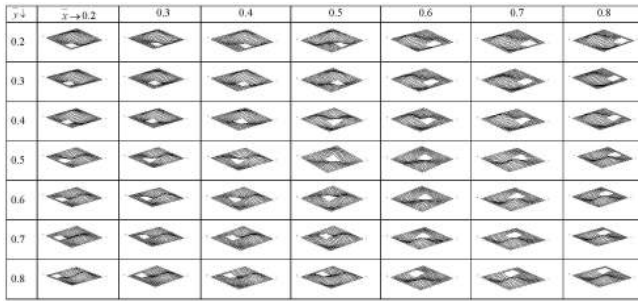


Figure 6: First mode shapes of laminated composite (0/90/0/90) stiffened elliptic parabolic shell for different position of the central square cutout and CCCC boundary condition

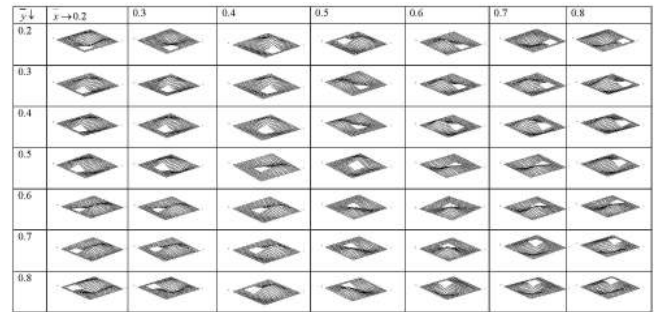


Figure 10: First mode shapes of laminated composite (+45/-45/+45/-45) stiffened elliptic parabolic shell for different position of the central square cutout and CCCC boundary condition.

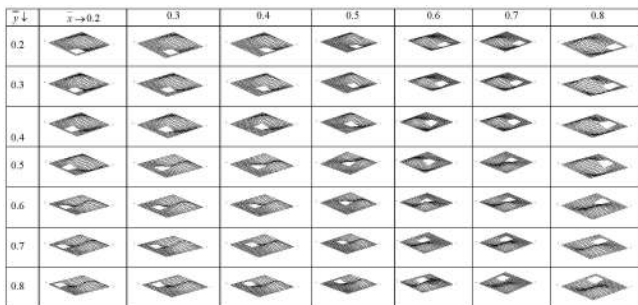


Figure 7: First mode shapes of laminated composite (0/90/0/90) stiffened elliptic parabolic shell for different position of the central square cutout and CCSC boundary condition.

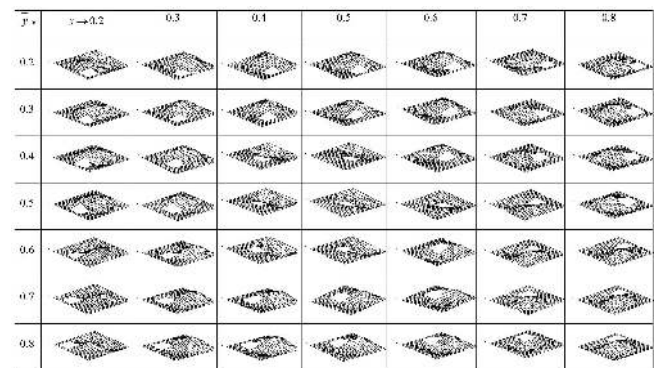


Figure 11: First mode shapes of laminated composite (+45/-45/+45/-45) stiffened elliptic parabolic shell for different position of the central square cutout and CCSC boundary condition.

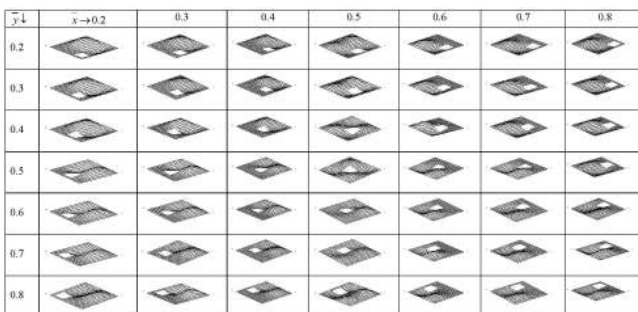


Figure 8: First mode shapes of laminated composite (0/90/0/90) stiffened elliptic parabolic shell for different position of the central square cutout and SCSC boundary condition.

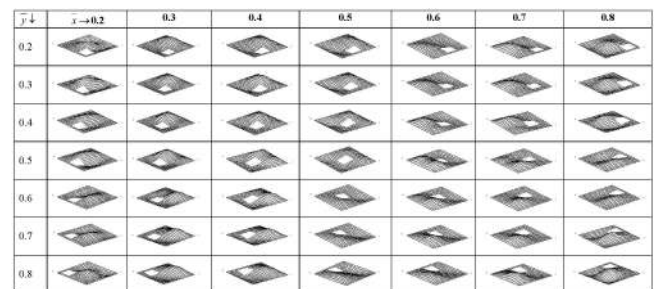


Figure 12: First mode shapes of laminated composite (+45/-45/+45/-45) stiffened elliptic parabolic shell for different position of the central square cutout and SCSC boundary condition.

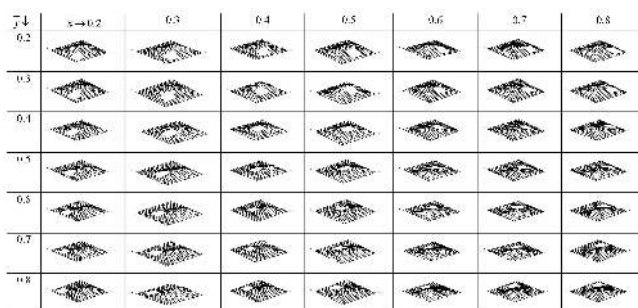


Figure 9: First mode shapes of laminated composite (0/90/0/90) stiffened elliptic parabolic shell for different position of the central square cutout and SSSC boundary condition.

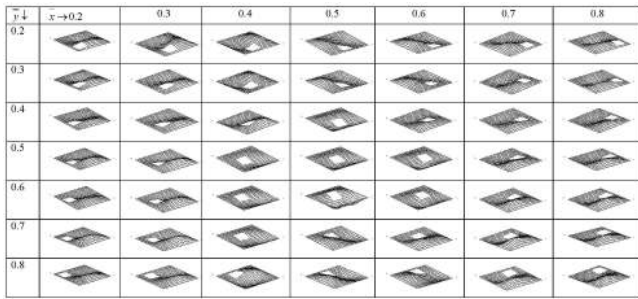


Figure 13: First mode shapes of laminated composite (+45/-45/+45/-45) stiffened elliptic parabolic shell for different position of the central square cutout and SSSC boundary condition.

Table 7: Values of ‘r’ for 0/90/0/90 elliptic parabolic shells.

Edge condition	\bar{y}	\bar{x}						
		0.2	0.3	0.4	0.5	0.6	0.7	0.8
CCCC	0.2	91.56	94.52	99.99	106.19	99.98	94.51	91.56
	0.3	90.17	92.97	98.13	104.72	98.14	92.97	90.17
	0.4	91.13	93.27	97.36	101.19	97.36	93.27	91.13
	0.5	92.77	94.26	97.32	100	97.32	94.25	92.76
	0.6	91.13	93.27	97.36	101.20	97.36	93.27	91.13
	0.7	90.17	92.97	98.13	103.92	98.14	92.97	90.17
	0.8	91.29	94.22	99.64	106.12	99.86	94.28	91.37
	CSCC	0.2	92.98	94.81	97.51	99.58	97.51	94.81
0.3		93.52	96.56	101.13	105.32	101.13	96.57	93.53
0.4		94.02	97.09	102.07	105.84	102.07	97.11	94.02
0.5		93.46	94.87	97.65	100	97.78	94.93	93.35
0.6		90.92	90.64	92.24	93.71	92.36	90.73	90.64
0.7		89.24	88.69	90.10	91.35	90.18	88.76	88.93
0.8		89.00	88.52	89.93	91.16	90.04	88.60	88.72
CCSC		0.2	83.73	86.74	92.51	102.51	107.23	98.91
	0.3	83.10	86.09	91.82	101.71	105.11	97.36	91.99
	0.4	83.06	85.73	91.07	100.59	103.21	95.04	89.13
	0.5	83.33	85.79	90.85	100	102.12	93.80	87.52
	0.6	83.06	85.73	91.07	100.59	103.20	95.04	89.13
	0.7	83.10	86.09	91.82	101.71	105.11	97.36	91.99
	0.8	83.54	86.53	92.27	102.40	107.14	98.67	92.98
	CCCS	0.2	88.91	88.75	90.14	91.28	90.14	88.75
0.3		89.07	88.87	90.26	91.45	90.26	88.87	89.07
0.4		90.80	90.83	92.40	93.76	92.40	90.83	90.80
0.5		93.57	95.08	97.82	100	97.82	95.08	93.57
0.6		94.25	97.34	102.31	106.1	102.31	97.34	94.25
0.7		93.76	96.80	101.39	105.58	101.39	96.80	93.76
0.8		92.19	94.34	97.46	99.75	97.51	94.51	92.39
CSSC		0.2	84.56	87.63	92.36	96.84	94.20	87.16
	0.3	88.23	91.68	96.61	101.01	99.45	93.40	87.01
	0.4	89.69	93.31	98.43	103.22	103.29	98.83	93.48
	0.5	86.68	89.50	94.15	100	101.47	97.52	92.85
	0.6	82.76	85.11	89.33	94.97	96.30	92.28	87.84
	0.7	80.45	82.72	86.63	91.35	92.16	88.72	84.83
	0.8	79.53	81.75	85.33	89.18	89.69	86.86	83.47
	CCSS	0.2	79.55	81.78	85.37	89.18	89.68	86.85
0.3		80.45	82.72	86.63	91.35	92.14	88.70	84.80
0.4		82.76	85.12	89.33	94.97	96.28	92.25	87.82
0.5		86.68	89.50	94.15	100	101.45	97.49	92.83
0.6		89.68	93.31	98.43	103.22	103.29	98.82	93.48
0.7		88.21	91.68	96.61	101.00	99.45	93.40	87.01
0.8		84.21	87.30	92.09	96.69	93.98	86.89	79.80
CSCS		0.2	89.93	89.24	88.60	88.27	88.60	89.24
	0.3	91.09	90.34	90.39	90.56	90.39	90.34	91.08
	0.4	93.18	93.05	93.91	94.69	93.91	93.05	93.19
	0.5	94.49	96.72	98.67	100	98.63	96.72	94.49
	0.6	93.18	93.05	93.91	94.69	93.91	93.05	93.19

Table 7: Continued

Edge condition	\bar{y}	\bar{x}						
		0.2	0.3	0.4	0.5	0.6	0.7	0.8
SCSC	0.7	91.08	90.34	90.39	90.56	90.39	90.34	91.07
	0.8	89.89	89.23	88.59	88.25	88.59	89.23	89.95
	0.2	82.72	86.72	93.25	102.59	93.25	86.72	82.72
	0.3	82.30	86.18	92.57	102.07	92.57	86.18	82.30
	0.4	80.76	84.77	91.12	101.41	91.12	84.77	80.76
	0.5	79.84	84.01	90.38	100	90.37	84.01	79.83
	0.6	80.76	84.77	91.12	101.52	91.12	84.77	80.76
	0.7	82.30	86.18	92.57	102.11	92.57	86.18	82.30
CSSS	0.8	82.54	86.52	93.02	102.52	93.18	86.58	82.62
	0.2	80.04	82.38	86.12	90.10	89.36	84.28	78.66
	0.3	82.65	85.07	89.04	93.53	93.52	88.86	83.63
	0.4	85.97	88.64	92.83	97.54	98.11	93.98	89.07
	0.5	88.38	91.49	95.81	100	100.72	97.45	93.21
	0.6	85.97	88.64	92.83	97.54	98.11	93.98	89.07
	0.7	82.65	85.07	89.04	93.53	93.52	88.86	83.63
	0.8	79.98	82.30	86.04	90.01	89.21	84.13	78.52
SSSC	0.2	80.54	86.67	93.10	97.09	93.12	86.67	80.54
	0.3	86.64	92.12	97.83	100.98	97.83	92.12	86.64
	0.4	90.77	95.33	100.28	102.88	100.28	95.33	90.77
	0.5	87.67	91.57	96.62	100	96.62	91.57	87.67
	0.6	83.52	87.06	91.84	95.36	91.84	87.06	83.52
	0.7	81.37	84.66	88.97	91.86	88.97	84.66	81.37
	0.8	80.62	83.74	87.56	89.85	87.57	83.74	80.64
	SSCS	0.2	78.66	84.28	89.36	90.10	86.12	82.37
0.3		83.63	88.86	93.52	93.53	89.04	85.07	82.65
0.4		89.07	93.98	98.11	97.54	92.83	88.64	85.97
0.5		93.20	97.44	100.72	100	95.81	91.49	88.38
0.6		89.07	93.98	98.11	97.54	92.83	88.64	85.97
0.7		83.63	88.86	93.52	93.53	89.04	85.08	82.65
0.8		78.56	84.17	89.24	90.04	86.04	82.30	79.97
SSSS		0.2	78.59	83.13	87.99	90.85	87.99	83.13
	0.3	82.32	86.55	91.32	94.19	91.32	86.55	82.32
	0.4	86.57	90.67	95.28	97.93	95.28	90.66	86.57
	0.5	89.92	93.81	97.93	100	97.93	93.81	89.92
	0.6	86.57	90.66	95.28	97.93	95.28	90.66	86.57
	0.7	82.32	86.55	91.32	94.19	91.32	86.55	82.32
	0.8	78.49	83.04	87.87	90.76	87.86	83.00	78.46
	CS	0.2	102.07	103.47	105.37	108.62	105.34	103.47
0.3		101.38	102.39	103.96	106.47	103.96	102.39	101.38
0.4		99.29	99.63	83.95	102.26	100.64	99.63	99.29
0.5		98.03	98.06	98.77	100	98.74	98.03	98.03
0.6		99.29	99.63	100.64	102.26	100.64	99.63	99.29
0.7		101.40	102.39	103.99	106.62	103.96	102.36	101.38
0.8		101.65	103.03	104.80	107.16	104.63	103.00	101.67

$a/b = 1, a/h = 100, a'/b' = 1, h/R_{xx} = 1/300, R_{xx}/R_{yy} = 1.5;$
 $E_{11}/E_{22} = 25, G_{23} = 0.2 E_{22}, G_{13} = G_{12} = 0.5 E_{22}, \nu_{12} = \nu_{21} = 0.25.$

Table 8: Values of 'r' for +45/-45/+45/-45 elliptic parabolic shells.

Edge condition	\bar{y}	\bar{x}						
		0.2	0.3	0.4	0.5	0.6	0.7	0.8
CCCC	0.2	79.66	82.85	84.84	85.74	84.86	82.87	79.69
	0.3	80.31	84.19	87.56	89.71	87.66	84.28	80.35
	0.4	80.05	84.59	90.03	95.29	90.17	84.67	80.08
	0.5	79.67	84.63	91.24	100	91.22	84.61	79.67
	0.6	80.09	84.67	90.19	94.95	90.06	84.59	80.08
	0.7	80.36	84.28	87.66	89.54	87.56	84.20	80.32
	0.8	79.57	82.84	84.84	85.66	84.87	82.81	79.57
	CSCC	0.2	97.21	99.98	103.64	107.41	103.36	99.85
0.3		97.50	103.57	108.60	109.94	108.48	103.37	97.07
0.4		92.15	97.10	102.06	104.71	102.12	96.68	91.33
0.5		87.35	91.82	96.90	100	96.91	91.46	86.53
0.6		87.12	91.38	96.09	98.75	95.98	91.19	86.61
0.7		89.41	93.62	97.54	99.38	97.34	93.61	89.28
0.8		89.58	94.39	98.14	99.38	98.18	94.80	89.75
CCSC		0.2	90.79	90.78	88.46	88.76	94.18	97.45
	0.3	92.55	92.96	91.44	92.48	98.49	99.29	93.22
	0.4	92.00	94.63	94.78	96.94	103.47	99.94	93.45
	0.5	91.54	96.78	97.42	100	106.45	100.15	93.66
	0.6	92.14	95.54	95.18	97.14	103.07	99.81	93.50
	0.7	92.21	93.32	91.74	92.90	98.85	99.17	93.24
	0.8	90.44	90.67	88.63	89.30	94.91	97.64	92.86
	CCCS	0.2	89.73	94.81	98.21	99.41	98.18	94.41
0.3		89.28	93.62	97.36	99.39	97.57	93.64	89.20
0.4		86.61	91.19	95.99	98.76	96.10	91.41	86.94
0.5		86.51	91.44	96.88	100	96.91	91.85	87.19
0.6		91.29	96.65	102.07	104.69	102.08	97.11	92.04
0.7		97.05	103.36	108.51	109.93	108.62	103.60	97.45
0.8		97.11	99.63	103.03	107.13	102.98	99.55	96.72
CSSC		0.2	96.07	97.95	96.72	98.01	101.80	100.96
	0.3	95.28	100.08	100.59	102.37	106.09	102.77	97.35
	0.4	90.75	95.97	101.16	104.11	102.58	97.75	92.51
	0.5	86.40	91.38	96.69	100	98.25	93.44	88.45
	0.6	86.00	90.90	95.98	98.98	97.24	92.86	87.83
	0.7	87.80	92.80	97.46	99.69	98.05	94.24	89.08
	0.8	87.80	92.74	95.59	96.69	98.21	94.82	89.48
	CCSS	0.2	87.45	92.91	95.60	95.95	98.42	94.43
0.3		87.26	92.71	97.53	99.91	98.29	94.11	88.91
0.4		84.96	90.37	95.92	99.20	97.19	92.68	87.80
0.5		84.85	90.37	96.37	100	97.75	93.00	88.27
0.6		89.04	94.69	100.51	103.81	101.83	97.06	92.14
0.7		94.10	99.54	100.63	102.25	106.26	102.45	97.05
0.8		94.40	97.96	96.84	98.09	101.74	100.69	96.82
CSCS		0.2	93.56	98.10	101.23	101.93	100.57	97.29
	0.3	93.52	97.73	101.01	102.31	100.96	97.51	93.28
	0.4	89.31	93.65	98.28	100.90	98.29	93.49	89.13

Table 8: Continued

Edge condition	\bar{y}	\bar{x}						
		0.2	0.3	0.4	0.5	0.6	0.7	0.8
SCSC	0.5	86.91	91.36	96.69	100	96.69	91.36	86.91
	0.6	89.13	93.49	98.29	100.90	98.28	93.65	82.77
	0.7	93.28	97.51	100.96	102.31	101.01	97.73	93.52
	0.8	92.92	97.13	100.29	101.59	100.83	97.83	93.46
	0.2	93.51	94.06	90.70	88.69	90.56	93.94	92.74
	0.3	94.58	96.25	93.72	92.19	93.76	96.61	93.70
	0.4	94.49	98.00	97.26	96.75	97.57	98.98	94.12
	0.5	94.44	100.09	99.96	100	99.96	100.04	94.44
CSSS	0.6	94.30	99.03	97.57	96.75	97.26	98.03	94.55
	0.7	93.72	96.62	93.76	92.19	93.72	96.25	94.58
	0.8	92.63	93.90	90.50	88.68	90.65	94.01	93.43
	0.2	92.34	97.05	99.89	102.08	101.06	97.11	92.43
	0.3	92.26	97.42	101.57	103.12	101.63	97.54	92.86
	0.4	88.26	93.24	98.33	101.33	99.72	95.24	90.48
	0.5	85.90	90.81	96.30	100	98.29	93.65	88.99
	0.6	87.98	92.83	97.85	100.79	99.22	94.97	90.35
SSSC	0.7	91.92	96.81	100.79	102.33	101.07	97.37	92.87
	0.8	91.86	96.25	99.20	101.30	100.71	97.26	92.76
	0.2	95.24	100.24	98.64	97.67	98.86	100.02	95.33
	0.3	94.79	100.29	102.55	102.03	102.87	99.87	94.26
	0.4	90.56	95.77	100.92	102.99	100.82	95.44	89.91
	0.5	86.98	92.26	97.33	100	97.48	92.02	86.40
	0.6	86.37	91.96	97.05	99.55	97.12	91.82	85.92
	0.7	87.23	93.18	98.30	99.97	98.31	93.23	87.05
SSCS	0.8	87.15	93.08	97.28	95.80	98.16	93.43	87.21
	0.2	92.91	97.63	101.14	101.82	99.56	96.53	91.98
	0.3	92.87	97.37	101.07	102.33	100.79	96.82	91.91
	0.4	90.35	94.97	99.22	100.79	97.85	92.83	87.98
	0.5	88.99	93.65	98.30	100	96.30	90.81	85.90
	0.6	90.48	95.24	99.72	101.33	98.32	93.24	88.26
	0.7	92.86	97.54	101.63	103.12	101.57	97.44	92.25
	0.8	92.25	96.84	100.73	102.03	99.38	96.74	92.22
SSSS	0.2	91.17	96.36	100.55	102.18	100.03	95.81	90.74
	0.3	91.11	96.35	100.87	102.54	100.75	96.14	90.94
	0.4	88.70	93.93	98.75	100.97	98.79	93.90	88.66
	0.5	87.30	92.47	97.51	100	97.51	92.47	87.30
	0.6	88.66	93.90	98.79	100.97	98.75	93.93	88.70
	0.7	90.94	96.14	100.75	102.54	100.87	96.35	91.11
	0.8	90.45	95.42	99.57	101.70	99.99	95.97	90.86
	CS	0.2	106.23	111.34	112.81	111.57	112.47	110.47
0.3		105.47	108.78	108.65	107.73	108.76	108.42	104.76
0.4		100.53	102.66	102.71	102.13	102.87	102.76	100.53
0.5		98.68	100.50	100.47	100	100.47	100.50	98.66
0.6		100.53	102.76	102.87	102.13	102.71	102.66	100.53
0.7		104.76	108.42	108.76	107.73	108.65	108.84	105.47
0.8		105.39	110.49	111.89	110.60	112.07	111.13	106.15

$$a/b = 1, a/h = 100, a'/b' = 1, h/R_{xx} = 1/300, R_{xx}/R_{yy} = 1.5;$$

Table 8: Continued

Edge condition	\bar{y}	\bar{x}						
	0.2	0.3	0.4	0.5	0.6	0.7	0.8	
$E_{11}/E_{22} = 25, G_{23} = 0.2 E_{22}, G_{13} = G_{12} = 0.5 E_{22}, \nu_{12} = \nu_{21} = 0.25.$								

Table 9: Maximum values of r with corresponding coordinates of cutout centres and zones where $r \geq 90$ and $r \geq 95$ for 0/90/0/90 elliptic parabolic shells.

Boundary Condition	Maximum values of r	Co-ordinate of cutout centre	Area in which the value of $r \geq 90$	Area in which the value $r \geq 95$
CCCC	106.18	$\bar{x} = 0.5$ $\bar{y} = 0.2$	$0.2 \leq \bar{x} \leq 0.3; 0.7 \leq \bar{x} \leq 0.8$ $0.2 \leq \bar{y} \leq 0.8$	$0.4 \leq \bar{x} \leq 0.5$ $0.2 \leq \bar{y} \leq 0.8$
CSCC	105.84	$\bar{x} = 0.5$ $\bar{y} = 0.4$	$0.2 \leq \bar{x} \leq 0.3; 0.7 \leq \bar{x} \leq 0.8$ $0.2 \leq \bar{y} \leq 0.6$ $0.4 \leq \bar{x} \leq 0.6, 0.6 \leq \bar{y} \leq 0.8$	$0.4 \leq \bar{x} \leq 0.6$ $0.2 \leq \bar{y} \leq 0.5$
CCSC	107.23	$\bar{x} = 0.6$ $\bar{y} = 0.2$	$\bar{x} = 0.4, 0.2 \leq \bar{y} \leq 0.8$	$0.5 \leq \bar{x} \leq 0.7$ $0.2 \leq \bar{y} \leq 0.8$
CCCS	106.12	$\bar{x} = 0.5$ $\bar{y} = 0.6$	$0.2 \leq \bar{x} \leq 0.3, 0.7 \leq \bar{x} \leq 0.8$ $0.2 \leq \bar{y} \leq 0.8;$ $0.4 \leq \bar{x} \leq 0.6, 0.2 \leq \bar{y} \leq 0.4$	$0.4 \leq \bar{x} \leq 0.6$ $0.5 \leq \bar{y} \leq 0.8$
CSSC	103.29	$\bar{x} = 0.6$ $\bar{y} = 0.4$	$\bar{x} = 0.4, 0.7, 0.2 \leq \bar{y} \leq 0.6;$ $0.5 \leq \bar{x} \leq 0.6, 0.6 \leq \bar{y} \leq 0.7$	$0.5 \leq \bar{x} \leq 0.6$ $0.3 \leq \bar{y} \leq 0.5$
CCSS	103.29	$\bar{x} = 0.6$ $\bar{y} = 0.6$	$\bar{x} = 0.4, 0.5 \leq \bar{y} \leq 0.8;$ $\bar{x} = 0.7, 0.4 \leq \bar{y} \leq 0.7;$	$0.5 \leq \bar{x} \leq 0.6$ $0.5 \leq \bar{y} \leq 0.7$
CSCS	100.00	$\bar{x} = 0.5$ $\bar{y} = 0.5$	$0.2 \leq \bar{x} \leq 0.8, 0.3 \leq \bar{y} \leq 0.4;$ $0.2 \leq \bar{x} \leq 0.8, 0.6 \leq \bar{y} \leq 0.7;$	$0.3 \leq \bar{x} \leq 0.7$ $\bar{y} = 0.5$
SCSC	102.59	$\bar{x} = 0.5$ $\bar{y} = 0.2$	$\bar{x} = 0.4, 0.6$ $0.2 \leq \bar{y} \leq 0.8$	$\bar{x} = 0.5$ $0.2 \leq \bar{y} \leq 0.8$
CSSS	100.72	$\bar{x} = 0.6$ $\bar{y} = 0.5$	$\bar{x} = 0.4, 0.7$ $0.4 \leq \bar{y} \leq 0.6$	$0.5 \leq \bar{x} \leq 0.6$ $0.4 \leq \bar{y} \leq 0.6$
SSSC	102.88	$\bar{x} = 0.5$ $\bar{y} = 0.4$	$\bar{x} = 0.3, 0.7$ $0.3 \leq \bar{y} \leq 0.5$	$0.4 \leq \bar{x} \leq 0.6$ $0.3 \leq \bar{y} \leq 0.5$
SSCS	100.72	$\bar{x} = 0.4$ $\bar{y} = 0.5$	$\bar{x} = 0.3, 0.6$ $0.4 \leq \bar{y} \leq 0.6$	$0.4 \leq \bar{x} \leq 0.5$ $0.4 \leq \bar{y} \leq 0.6$
SSSS	100.00	$\bar{x} = 0.5$ $\bar{y} = 0.5$	$\bar{x} = 0.3, 0.7$ $0.4 \leq \bar{y} \leq 0.6$	$0.4 \leq \bar{x} \leq 0.6$ $0.4 \leq \bar{y} \leq 0.6$
CS	108.62	$\bar{x} = 0.5$ $\bar{y} = 0.2$	nil nil	$0.2 \leq \bar{x} \leq 0.8$ $0.2 \leq \bar{y} \leq 0.8$

$a/b = 1, a/h = 100, a'/b' = 1, h/R_{xx} = 1/300, R_{xx}/R_{yy} = 1.5;$
 $E_{11}/E_{22} = 25, G_{23} = 0.2 E_{22}, G_{13} = G_{12} = 0.5 E_{22}, \nu_{12} = \nu_{21} = 0.25.$

Table 10: Maximum values of r with corresponding coordinates of cutout centres and zones where $r \geq 90$ and $r \geq 95$ for +45/-45/+45/-45 elliptic parabolic shells.

Boundary Condition	Maximum values of r	Coordinate of cutout centre	Area in which value of $r \geq 90$	Area in which the value $r \geq 95$
CCCC	100.00	$\bar{x} = 0.5, \bar{y} = 0.5$	$\bar{x} = 0.4, 0.6, 0.4 \leq \bar{y} \leq 0.6$	$\bar{x} = 0.5, 0.4 \leq \bar{y} \leq 0.5$
CSCC	109.94	$\bar{x} = 0.5$ $\bar{y} = 0.3$	$\bar{x} = 0.3, 0.7$ $0.5 \leq \bar{y} \leq 0.8$	$0.2 \leq \bar{x} \leq 0.8, 0.2 \leq \bar{y} \leq 0.3$; $0.4 \leq \bar{x} \leq 0.6, 0.4 \leq \bar{y} \leq 0.8$;
CCSC	106.45	$\bar{x} = 0.$ $\bar{y} = 0.5$	$\bar{x} = 0.2, 0.8$ $0.2 \leq \bar{y} \leq 0.8$	$0.3 \leq \bar{x} \leq 0.4, 0.5 \leq \bar{y} \leq 0.6$; $\bar{x} = 0.5, 0.4 \leq \bar{y} \leq 0.6$; $\bar{x} = 0.6, 0.3 \leq \bar{y} \leq 0.7$; $\bar{x} = 0.7, 0.2 \leq \bar{y} \leq 0.8$;
CCCS	109.93	$\bar{x} = 0.5$ $\bar{y} = 0.7$	$\bar{x} = 0.3, 0.7$ $0.2 \leq \bar{y} \leq 0.5$	$0.4 \leq \bar{x} \leq 0.6, 0.2 \leq \bar{y} \leq 0.6$; $0.2 \leq \bar{x} \leq 0.8, 0.7 \leq \bar{y} \leq 0.8$
CSSC	106.09	$\bar{x} = 0.6$ $\bar{y} = 0.3$	$\bar{x} = 0.3, 0.7$ $0.5 \leq \bar{y} \leq 0.8$	$0.2 \leq \bar{x} \leq 0.8, 0.2 \leq \bar{y} \leq 0.3$; $0.4 \leq \bar{x} \leq 0.6, 0.4 \leq \bar{y} \leq 0.8$
CCSS	103.81	$\bar{x} = 0.5$ $\bar{y} = 0.6$	$\bar{x} = 0.3, 0.7$ $0.2 \leq \bar{y} \leq 0.6$	$0.4 \leq \bar{x} \leq 0.6, 0.2 \leq \bar{y} \leq 0.6$; $0.3 \leq \bar{x} \leq 0.8, 0.7 \leq \bar{y} \leq 0.8$
CSCS	102.31	$\bar{x} = 0.5$ $\bar{y} = 0.7$	$\bar{x} = 0.3, 0.7$ $0.4 \leq \bar{y} \leq 0.6$	$0.3 \leq \bar{x} \leq 0.7, 0.2 \leq \bar{y} \leq 0.3$ $\& 0.7 \leq \bar{y} \leq 0.8$; $0.4 \leq \bar{x} \leq 0.6, 0.4 \leq \bar{y} \leq 0.6$
SCSC	100.04	$\bar{x} = 0.7$ $\bar{y} = 0.5$	$\bar{x} = 0.2, 0.8$ $0.2 \leq \bar{y} \leq 0.8$	$\bar{x} = 0.3, 0.7, 0.3 \leq \bar{y} \leq 0.7$; $0.4 \leq \bar{x} \leq 0.6, 0.4 \leq \bar{y} \leq 0.6$
CSSS	103.12	$\bar{x} = 0.5$ $\bar{y} = 0.3$	$\bar{x} = 0.3, 0.7$ $0.4 \leq \bar{y} \leq 0.8$	$0.3 \leq \bar{x} \leq 0.7, 0.2 \leq \bar{y} \leq 0.3$; $0.4 \leq \bar{x} \leq 0.6, 0.4 \leq \bar{y} \leq 0.8$
SSSC	102.99	$\bar{x} = 0.5$ $\bar{y} = 0.4$	$\bar{x} = 0.3, 0.7$ $0.5 \leq \bar{y} \leq 0.8$	$0.3 \leq \bar{x} \leq 0.7, 0.2 \leq \bar{y} \leq 0.4$; $0.4 \leq \bar{x} \leq 0.6, 0.5 \leq \bar{y} \leq 0.8$
SSCS	103.12	$\bar{x} = 0.5$ $\bar{y} = 0.7$	$\bar{x} = 0.3, 0.7, 0.4 \leq \bar{y} \leq 0.6$; $\bar{x} = 0.2, 0.8, 0.2 \leq \bar{y} \leq 0.3$ & $0.7 \leq \bar{y} \leq 0.8$	$0.3 \leq \bar{x} \leq 0.7, 0.2 \leq \bar{y} \leq 0.3$ $\& 0.7 \leq \bar{y} \leq 0.8$; $0.4 \leq \bar{x} \leq 0.6, 0.4 \leq \bar{y} \leq 0.6$
SSSS	102.54	$\bar{x} = 0.5$ $\bar{y} = 0.7$	$\bar{x} = 0.3, 0.7$ $0.4 \leq \bar{y} \leq 0.6$; $\bar{x} = 0.2, 0.8$ $0.2 \leq \bar{y} \leq 0.3$ & $0.7 \leq \bar{y} \leq 0.8$	$0.3 \leq \bar{x} \leq 0.7, 0.2 \leq \bar{y} \leq 0.3$ $\& 0.7 \leq \bar{y} \leq 0.8$; $0.4 \leq \bar{x} \leq 0.6, 0.4 \leq \bar{y} \leq 0.6$
CS	112.47	$\bar{x} = 0.6$ $\bar{y} = 0.2$	nil	$0.2 \leq \bar{x} \leq 0.8$ $0.2 \leq \bar{y} \leq 0.8$

$a/b = 1, a/h = 100, a'/b' = 1, h/R_{xx} = 1/300, R_{xx}/R_{yy} = 1.5$;
 $E_{11}/E_{22} = 25, G_{23} = 0.2 E_{22}, G_{13} = G_{12} = 0.5 E_{22}, \nu_{12} = \nu_{21} = 0.25.$

The laminated composite finite element shell model proposed in the present study can work also with anisotropic lamination with general orientation of the plies. However, the present study considers only cross-ply and angle-ply lamination schemes. Future studies will consider anisotropic laminations.

4 Conclusions

The following conclusions may be drawn from the present study:

1. This approach is suitable for analyzing free vibration problems of stiffened elliptic parabolic shell panels with cutouts. The finite element code used here produces results in close agreement with those of the benchmark problems.
2. The arrangement of boundary constraints along the four edges is far more important than their actual number as for free vibration is concerned.
3. If a fully clamped shell is released for any functional reason, then two alternate edges must release instead of two adjacent edges.
4. The relative free vibration performances of stiffened shells with cutout for different boundary combination are expected to be very helpful for practicing engineers.
5. For cross ply shells eccentricity towards the simply supported edge which is opposite to a clamped edge is preferable. For angle ply shells eccentricity towards simply supported edge is preferable.
6. This study may be helpful as design aids for structural engineers as it provides information regarding the behavior of stiffened elliptic parabolic shell with eccentric cutouts for a wide spectrum of eccentricity and boundary conditions for cross ply and angle ply shells.
7. That will also help an engineer to make a decision regarding the eccentricity of the cutout centre that he can allow as it provides information regarding the specific zones within which the cutout centre may be moved so that the loss of frequency is less than 10% with respect to a shell with a central cutout.

References

- [1] Ghosh B., Bandyopadhyay J.N., Analysis of Paraboloidal of Revolution Type Shell Structures using Isoparametric Doubly Curved Shell Elements, *Comput. Struct.*, 1990, 36(5), 791-800.
- [2] Dey A., Bandyopadhyay J.N., Sinha P.K., Finite Element Analysis of Laminated Composite Paraboloidal of Revolution shells, *Comput. Struct.*, 1992, 44(3), 675-682.
- [3] Dey A., Bandyopadhyay J.N., Sinha P.K., Behaviour of Paraboloidal of Revolution Shell using Cross-ply and Anti-symmetric Angle-ply Laminates, *Comput. Struct.*, 1994, 52(6), 1301-1308.
- [4] Chakravorty D., Sinha P.K., Bandyopadhyay J.N., Free Vibration Analysis of Point Supported Laminated Composite Doubly Curved Shells- A Finite Element Approach, *Comput. Struct.*, 1995, 54(2), 191-207.
- [5] Chakravorty D., Sinha P.K., Bandyopadhyay J.N., Finite Element Free Vibration Analysis of Doubly Curved Laminated Composite Shells, *J. Sound and Vibration*, 1996, 191(4), 491-504.
- [6] Nayak A.N., Bandyopadhyay J.N., Free Vibration Analysis and Design Aids of Stiffened Conoidal Shells, *J. Eng. Mech.*, 2002, 128, 419-427.
- [7] Nayak A.N., Bandyopadhyay J.N., Free Vibration Analysis of Laminated Stiffened Shells, *J. Eng. Mech.*, 2005, 131, 100-105.
- [8] Nayak A.N., Bandyopadhyay J.N., Dynamic Response Analysis of Stiffened Conoidal Shells, *J. Sound and Vibration*, 2006, 291, 1288-1297.
- [9] Das H.S., Chakravorty D., Design Aids and Selection Guidelines for Composite Conoidal Shell Roofs-A Finite Element Application, *J. Reinforced Plastic and Composites*, 2007, 26, 1793-1819.
- [10] Das H.S., Chakravorty D., Natural Frequencies and Mode Shapes of Composite Conoids with Complicated Boundary Conditions, *J. Reinforced Plastic and Composites*, 2008, 27, 1397-1415.
- [11] Das H.S., Chakravorty D., Finite Element Application in Analysis and Design of Point Supported Composite Conoidal Shell Roofs Suggesting Selection Guidelines, *J. Strain Analysis in Eng. Design*, 2010, 45(3), 165-177.
- [12] Das H.S., Chakravorty D., Bending Analysis of Stiffened Composite Conoidal Shell Roofs Through Finite Element Application, *J. Compos. Mater.*, 2011, 45, 525-542.
- [13] Pradyumna S., Bandyopadhyay J.N., Static and Free Vibration Analyses of Laminated Shells using A Higher Order Theory, *J. Reinforced Plastics and Composites*, 2008, 27, 167-186.
- [14] Pradyumna S., Bandyopadhyay J.N., Dynamic Instability Behaviour of Laminated Hypar and Conoid Shells using A Higher-Order Shear Deformation Theory, *Thin Walled Struct.*, 2011, 49, 77-84.
- [15] Reddy J.N., Large Amplitude Flexural Vibration of Layered Composite Plates with Cutouts, *J. Sound and Vibration*, 1982, 83(1), 1-10.
- [16] Malhotra S.K., Ganesan N., Veluswami M.A., Vibration of Composite Plate with Cutouts, *J. Aeronautical Soc. India*, 1989, 41, 61-64.
- [17] Sivasubramanian B., Kulkarni A.M., Rao G.V., Krishnan A., Free Vibration of Curved Panels with Cutouts, *J. Sound and Vibration*, 1997, 200(2), 227-234.
- [18] Sivakumar K., Iyengar N.G.R., Deb K., Free Vibration of Laminated Composite Plates with Cutout, *J. Sound and Vibration*, 1999, 221(3), 443-465.
- [19] Rossi R.E., Transverse Vibrations of Thin, Orthotropic Rectangular Plates with Rectangular Cutouts with Fixed Boundaries, *J. Sound and Vibration*, 1999, 221(4), 733-736.
- [20] Huang M., Sakiyama T., Free Vibration Analysis of Rectangular Plates with Various-Shaped Holes, *J. Sound and Vibration*,

- 1999, 226(4), 769-786.
- [21] Hota S.S., Padhi P., *Vibration of Plates with Arbitrary Shapes of Cutouts*, *J. Sound and Vibration*, 2007, 302(4-5), 1030-1036.
- [22] Chakravorty D., Sinha P.K., Bandyopadhyay J.N., *Applications of FEM on Free and Forced Vibration of Laminated Shells*, *J. Eng. Mech.*, 1998, 124(1), 1-8.
- [23] Sivasubramonian B., Rao G.V., Krishnan A., *Free Vibration of Longitudinally Stiffened Curved Panels with Cutout*, *J. Sound and Vibration*, 1999, 226(1), 41-55.
- [24] Hota S.S., Chakravorty D., *Free Vibration of Stiffened Conoidal Shell Roofs with Cutouts*, *J. Vibration and Control*, 2007, 13(3), 221-240.
- [25] Nanda N., Bandyopadhyay J.N., *Nonlinear Free Vibration Analysis of Laminated Composite Cylindrical Shells with Cutouts, J. Reinforced Plastic and Composites*, 2007, 26(14), 143-1427.
- [26] Qatu M.S., Sullivan R. W., Wang W., *Recent Research Advances on The Dynamic Analysis of Composite Shells: 2000-2009*, *Compos. Struct.*, 2010, 93, 14-31.
- [27] Kumar A., Chakrabarti A., Bhargava P., *Finite Element Analysis of Laminated Composite and Sandwich Shells using Higher Order Zigzag Theory*, *Compos. Struct.*, 2013, 106, 270-281.
- [28] Kumar A., Chakrabarti A., Bhargava P., *Vibration of Laminated Composites and Sandwich Shells Based on Higher Order Zigzag Theory*, *Eng. Struct.*, 2013, 56, 880-888.
- [29] Kumar A., Chakrabarti A., Bhargava P., *Vibration of Laminated Composite Shells with Cutouts using Higher Order Shear Deformation Theory*, *Int. J. Sci. Eng. Res.*, 2013, 4(5), 199-202.
- [30] Kumar A., Chakrabarti A., Bhargava P., *Accurate Dynamic Response of Laminated Composites and Sandwich Shells using Higher Order Zigzag Theory*, *Thin Walled Struct.*, 2014, 77, 174-186.
- [31] Ye T., Jin G., Chen Y., Ma X., Su Z., *Free Vibration Analysis of Laminated Composite Shallow Shells with General Elastic Boundaries*, *Compos. Struct.*, 2013, 106, 470-490.
- [32] Ye T., Jin G., Chen Y., Shi S., *A Unified Formulation for Vibration Analysis of Open Shells with Arbitrary Boundary Conditions*, *Int. J. Mech. Sci.*, 2014, 81, 42-59.
- [33] Jin G., Ye T., Jia X., Gao S., *A General Fourier Solution for The Vibration Analysis of Composite Laminated Structure Elements of Revolution with General Elastic Restraints*, *Compos. Struct.*, 2014, 109, 150-168.
- [34] Ye T., Jin G., Su Z., Jia X., *A Unified Chebyshev-Ritz Formulation for Vibration Analysis of Composite Laminated Deep Open Shells with Arbitrary Boundary Conditions*, *Arch. Appl. Mech.*, 2014, 84, 441-471.
- [35] Tornabene F., Fantuzzi N., Baccocchi M., *The Local GDQ Method Applied to General Higher-Order Theories of Doubly-Curved Laminated Composite Shells and Panels: The Free Vibration Analysis*, *Compos. Struct.*, 2014, 116, 637-660.
- [36] Tornabene F., Fantuzzi N., Viola E., Reddy J.N., *Winkler-Pasternak Foundation Effect on the Static and Dynamic Analyses of Laminated Doubly-Curved and Degenerate Shells and Panels*, *Composites Part B Eng.*, 2014, 57(1), 269-296.
- [37] Tornabene F., Viola E., Fantuzzi N., *General Higher-order Equivalent Single Layer Theory for Free Vibrations of Doubly-Curved Laminated Composite Shells and Panels*, *Compos. Struct.*, 2013, 104(1), 94-117.
- [38] Natarajan S., Ferreira A.J.M., Nguyen-Xuan H., *Analysis of Cross-Ply Laminated Plates using Isogeometric Analysis and Unified Formulation*, *Curved and Layered Structures*, 2014, 1, 1-10
- [39] Nanda N., Bandyopadhyay J.N., *Large Amplitude Free Vibration of Laminated Composite Shells with Cutout*, *Aircraft Eng. Aerospace Tech.*, 2008, 80(2), 165-174.
- [40] Nanda N., Bandyopadhyay J.N., *Nonlinear Transient Response of Laminated Composite Shells*, *J. Eng. Mech.*, 2008, 134(11), 983-990.
- [41] Brischetto S., Torre R., *Exact 3D Solutions and Finite Element 2D Models for Free Vibration Analysis of Plates and Cylinders, Curved and Layered Structures*, 2014, 1, 59-92.
- [42] Sahoo S., *Behaviour and Optimization Aids of Composite Stiffened Hypar Shell Roofs with Cutout under Free Vibration*, *ISRN Civil Eng.*, 2012, Article ID 989785, 1-14.
- [43] Sahoo S., *Free Vibration of Laminated Composite Hypar Shell Roofs with Cutouts*, *Advances in Acoustics and Vibrations*, 2011, Article ID 403684, 1-13.
- [44] Ghazijahani T.G., Jiao H., Holloway D., *Structural Behavior of Shells with Different Cutouts under Compression: An Experimental Study*, *J. Constructional Steel Res.*, 2015, 105, 129-137
- [45] Mohazzab A.H., Dozio L., *Prediction of Natural Frequencies of Laminated Curved Panels using Refined 2-D Theories in The Spectral Collocation Method*, *Curved and Layered Structures*, 2015, 2, 1-14.
- [46] Sai Ram K.S., Sreedhar Babu T., *Study of Bending of Laminated Composite Shells. Part II: Shells with A Cutout*, *Compos. Struct.*, 2001, 51(1), 117-126.
- [47] Fazzolari F.A., *A Refined Dynamic Stiffness Element for Free Vibration Analysis of Cross-Ply Laminated Composite Cylindrical and Spherical Shallow Shells*, *Composites Part B: Eng.*, 2014, 62, 143-158.
- [48] Vasiliev V.V., Jones R.M., Man L.L., *Mechanics of Composite Structures*, Taylor and Francis, USA, 1993.
- [49] Qatu M.S., *Vibration of Laminated Shells and Plates*, Elsevier, UK, 2004.
- [50] Dey A., Bandyopadhyay J.N., Sinha P.K., *Finite Element Analysis of Laminated Composite Paraboloidal of Revolution Shells*, *Comput. Struct.*, 1992, 44(3), 675-682.
- [51] Sahoo S., Chakravorty D., *Stiffened Composite Hypar Shell Roofs under Free Vibration: Behaviour and Optimization Aids*, *J. Sound and Vibration*, 2006, 295, 362-377.
- [52] Mukherjee A., Mukhopadhyay M., *Finite Element Free Vibration of Eccentrically Stiffened Plates*, *Comput. Struct.*, 1998, 30, 1303-1317.
- [53] Nayak A.N., Bandyopadhyay J.N., *On The Free Vibration of Stiffened Shallow Shells*, *J. Sound and Vibration*, 2002, 255(2), 357-382.